

## A STUDY ON THE SOFT MAGNETIC PROPERTIES OF Fe-Ta-(N,C) NANOCRYSTALLINE THIN FILMS

Dong-Hoon Shin, \*Dong-Hoon Ahn, Hyoung-June Kim, Seung-Eui Nam

Dep't of Metallurgy & Material Science, Hong-Ik University

72-1, Sangsu-Dong, Mapo-Gu, Seoul 121-791, Korea

\*Dep't of Image & Media Lab, LG electronics

16, Woomyeon-Dong, Seocho-Gu, Seoul, 137-140, Korea

**ABSTRACT:** Magnetic properties of FeTaN and FeTaC films deposited by DC magnetron reactive sputter were investigated, and correlated with their microstructures. The optimum magnetic properties of  $H_c : 0.25$  Oe,  $B_s : 14.5$  kG, and  $\mu' : 4000$  (5MHz) are observed in the  $Fe_{78.8}Ta_{8.5}N_{12.7}$  film, and  $H_c : 0.25$  Oe,  $B_s : 14.5$  kG, and  $\mu' : 2700$  (5MHz) in the  $Fe_{75.6}Ta_{8.1}C_{16.3}$  film. In both FeTaN and FeTaC films with minimum grain size show the best soft magnetic properties. Thermal stability of the soft magnetic properties of FeTaN is found to be higher than FeTaC for similar compositions. TaN and TaC particles form to retard the growth of  $\alpha$ -Fe grains. TaN particles in FeTaN films show higher efficiency in retarding the grain growth during heat treatments resulting the higher thermal stability, compared to TaC particles in FeTaC films.

### I. INTRODUCTIONS

MIG type magnetic recording heads require the soft magnetic films with high magnetic flux density. Recently, Fe-based nanocrystalline films have been reported to have high saturation magnetization as well as good soft magnetic properties[1~3]. Nanocrystalline microstructures can be realized by adding N or C with nitrides or carbides forming transition metal elements(e.g., Zr, Nb, Ta, Hf). These alloying elements forms fine nitrides or carbides particles in the Fe matrix, suppressing the grain growth of  $\alpha$ -Fe grains during the post-deposition heat treatments[4,5].

Generally, the films with C addition are known to have higher efficiency in retarding  $\alpha$ -Fe grain growth, thus leading to better magnetic properties and higher thermal stabilities, compared to the films with N addition. However, comprehensive studies on the difference in the film microstructures and magnetic properties between FeTaN and FeTaC films have not been reported. In this study, we investigated the microstructural evolutions and magnetic properties of FeTaN and FeTaC films, which are known to have good magnetic properties, to make a direct comparison between two films.

### II. EXPERIMENTS

FeTa(C or N) films with  $1 \mu m$  thickness were deposited by DC magnetron reactive sputtering apparatus. Ta compositions were changed by changing the area of Ta chips on the  $4''$  Fe target. N or C contents in the films were controlled by partial pressure of  $N_2$  or  $CH_4$  gases. The initial pressure was  $1 \times 10^{-6}$  Torr, and the working pressure was fixed at 1.5 mTorr. The  $N_2$  or  $CH_4$  partial pressure( $P_r$ ) was changed at  $0 \sim 0.3$  mTorr( $P_r/P_r+P_{Ar}=0 \sim 20\%$ ). The DC power was 420V, 0.47~0.48A and deposition rates were  $500 \sim 600 \text{ \AA}/min$ , which slightly depended on reactive gas partial pressure.

Glass (Corning #7059) was used as a substrate, which was water-cooled during deposition. Deposited samples were vacuum-annealed ( $5 \times 10^{-5}$  Torr) for 30 mins from  $400^\circ C$  to  $700^\circ C$ . The film compositions were analyzed by Auger electron spectroscopy calibrated with a standard sample. The formation of phases and grain sizes in the films after heat treatments was investigated by X-ray diffraction and TEM studies. The coercivity ( $H_c$ ) and saturation magnetization ( $4\pi M_s$ ) were measured by B-H loop tracer and VSM(Vibrating Sample Magnetometer), and the effective permeability was measured using the

Figure-8 coil method.

III.RESULTS AND DISCUSSION

Fig. 1. shows the  $4\pi M_s$  and  $H_c$  values of FeTaN and FeTaC films annealed at  $500^\circ\text{C}$  as a function of the reactive gas partial pressure. For FeTaN films,  $4\pi M_s$  decreases from

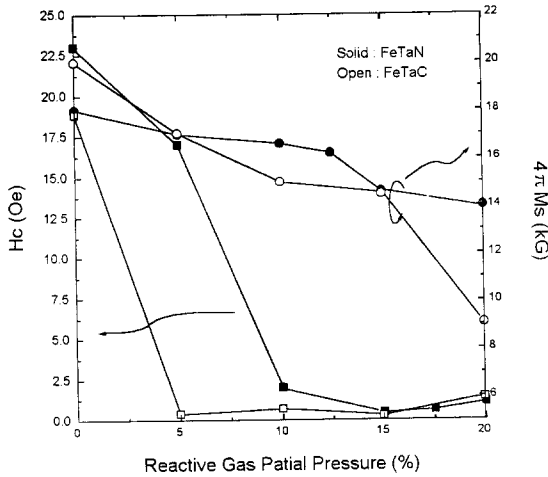


Fig. 1. Change of  $H_c$  and  $4\pi M_s$  as a function of the reactive gas partial pressure.

18 kG to 14 kG with increasing  $P_{N_2}$ .  $H_c$  decreases with  $P_{N_2}$  to the minimum value 0.25 Oe at  $P_{N_2}$  of 15~17%, then slightly increases at higher  $P_{N_2}$ . For FeTaC films, similarly to FeTaN films,  $4\pi M_s$  decreases with an increase of  $P_{CH_4}$ . High  $4\pi M_s$  above 14.5 kG can be obtained at  $P_{CH_4}$  up to 12.5%. The  $H_c$  more rapidly decreases with  $P_{CH_4}$  than FeTaN films and reaches the minimum values of 0.25~0.5 Oe at the  $P_{CH_4}$  of 5~15%. The process range showing minimum  $H_c$  appears to be larger in FeTaC than in FeTaN.

The behavior of  $H_c$  can be explained in terms of  $\alpha$ -Fe grain sizes in annealed films. The average grain sizes, determined by FWHM with  $\alpha$ -Fe (110) peaks of XRD, are plotted as a function of reactive gas partial pressure in Fig. 2. For FeTaN films, the average grain sizes slowly decrease with partial pressure and reach minimum grain sizes about 50 Å at 15%, at which films show the minimum  $H_c$ . On the other hand, in FeTaC films, grain sizes rapidly decrease to the minimum value at 5%, without significant changes for further increase in  $CH_4$  partial pressure. This result indicates that C addition is more effective in refining grain sizes than N addition.

The effective permeability ( $\mu'$ ) of 5 MHz for FeTaN and FeTaC films annealed at  $500^\circ\text{C}$  is plotted against various reactive gas partial pressures in Fig. 3. The

behavior of change of  $\mu'$  is found to be closely related

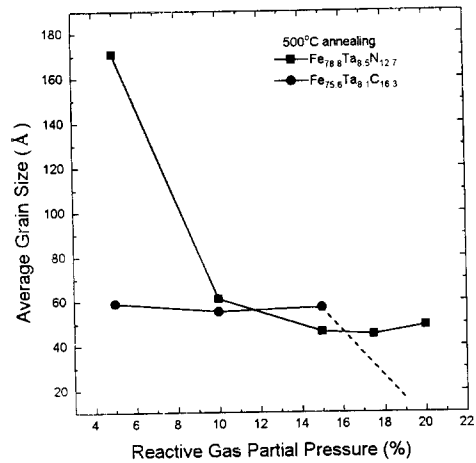


Fig. 2. Change of average grain size as a function of the reactive gas partial pressure.

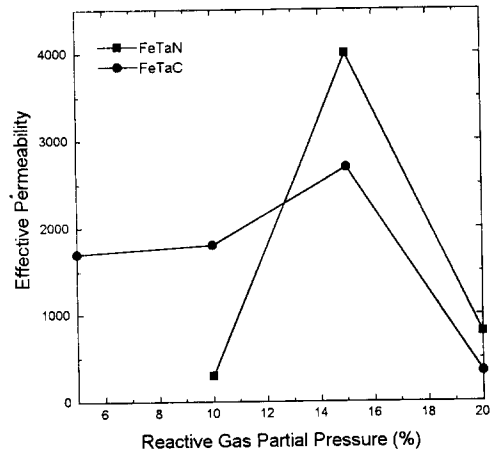


Fig. 3. Change of effective permeability as a function of the reactive gas partial pressure.

with the  $H_c$  value in both films, in that the films with low  $H_c$  show high  $\mu'$ . The  $\mu'$  increases with partial pressure and shows the maximum value at 15% in both FeTaN and FeTaC films. The maximum value of  $\mu'$  is 4000 in FeTaN films, which is higher than that of FeTaC films (2700). The best soft magnetic properties (FeTaN;  $4\pi M_s$ : 15 kG,  $H_c$ : 0.25 Oe, and  $\mu'$ : 4000, FeTaC;  $4\pi M_s$ : 14 kG,  $H_c$ : 0.25 Oe, and  $\mu'$ : 2700) are obtained at partial pressure of 15% in both FeTaN and FeTaC films, and corresponding film compositions are  $Fe_{78.8}Ta_{8.5}N_{12.7}$  and  $Fe_{75.6}Ta_{8.1}C_{16.3}$ .

respectively.

Dependence of  $\mu'$  on frequency was investigated for the films with best soft magnetic properties as shown in Fig. 4. While Fe<sub>75.6</sub>Ta<sub>8.1</sub>C<sub>16.3</sub> film shows slightly lower

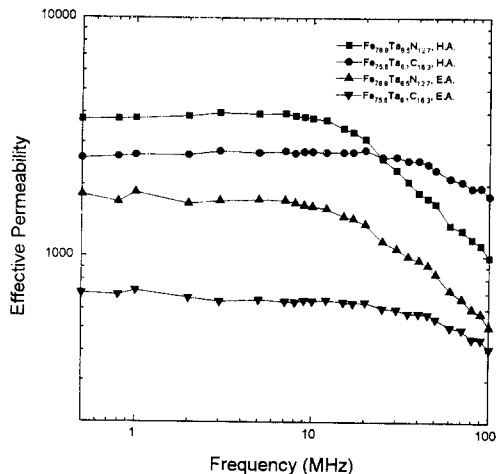


Fig. 4. Dependency of effective permeability on frequency for FeTaN and FeTaC films.

$\mu'$  value and better high frequency characteristics, compared with Fe<sub>78.8</sub>Ta<sub>8.5</sub>N<sub>12.7</sub> film. The  $\mu'$  of Fe<sub>75.6</sub>Ta<sub>8.1</sub>C<sub>16.3</sub> film sustains up to the frequency as high as 60 MHz.

The changes of magnetic properties of FeTaN(orC) films for various annealing temperatures are shown in Fig. 5.

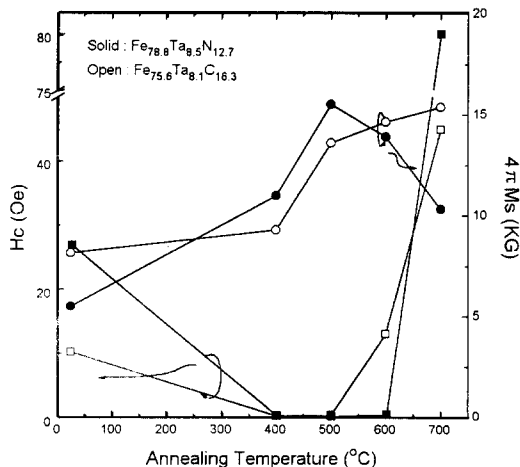


Fig. 5. Change of Hc and  $4\pi Ms$  as a function of the annealing temperature.

While FeTaN films show the maximum  $4\pi Ms$  at 500°C,

FeTaC films show a continuous increase of  $4\pi Ms$  up to 700°C. The Hc of films is lowered to the minimum value at 400°C in both films. As can be seen, rapid degradation of Hc is observed above 500°C and 600°C for FeTaC and FeTaN, respectively. Similar results are observed in the investigation of  $\mu'$  as shown in Fig. 6. Higher thermal stability of  $\mu'$  is observed in the FeTaN films.

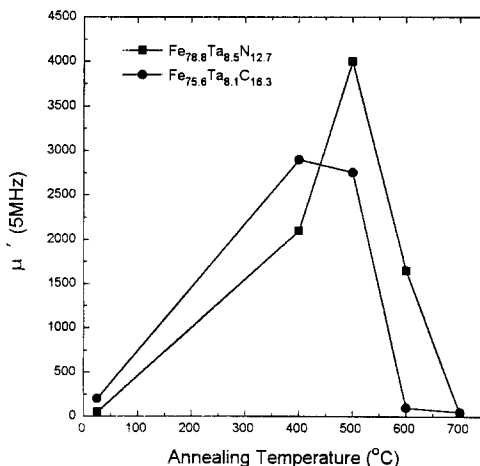
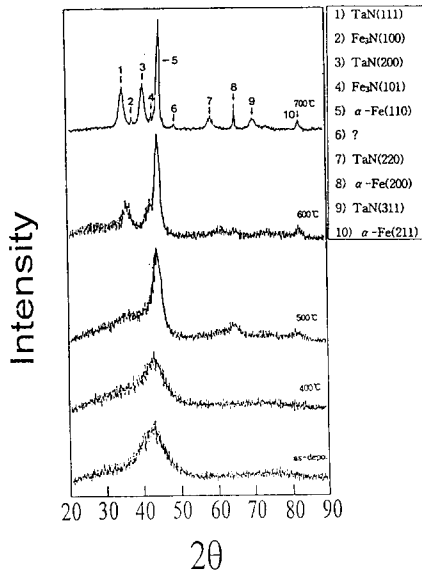


Fig. 6. Change of effective permeability as a function of the annealing temperature.

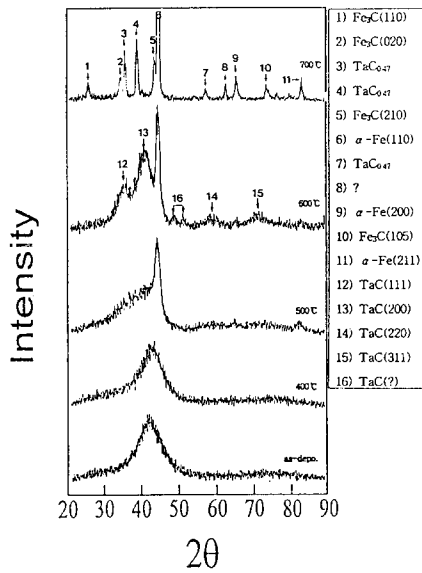
The superior thermal stability of FeTaN is somewhat in contrast with the reports that the C-added films have higher thermal stabilities than N-added films. Microstructural changes of annealed films were investigated by XRD, and the results are shown in Fig. 7. As shown in Fig. 7.(a), as-deposited FeTaN films have amorphous structures, which hold up to 400°C. Crystallization occurs at 500°C, showing the strong  $\alpha$ -Fe (110) textures. The broadening of the  $\alpha$ -Fe (110) peaks could result from the particle size effects (Scherrer effects) and non-uniform expansion of BCC lattice of  $\alpha$ -Fe with supersaturated N atoms. Asymmetrical peak shape with preferential broadening toward low diffraction angle (or higher interplanar distance) indicates that the lattice expansion. It may be the major cause of the apparent peak broadening. At 600°C, Fe<sub>3</sub>N peaks are shown near  $\alpha$ -Fe (110) peaks. The Fe<sub>4</sub>N or Fe<sub>2</sub>N phases, which are known to be the stable phases in the Fe-N phase diagrams, are not observed here[6]. The formation of Fe<sub>3</sub>N may be related to the transient phase transformation of the supersaturated  $\alpha$ -Fe phases. At 700°C, sharply defined  $\alpha$ -Fe, TaN, Fe<sub>3</sub>N peaks are observed indicating the growth of these phases.

Similar behavior of microstructural changes is observed in FeTaC films, as shown in Fig. 7.(b). Apparent crystallization of amorphous FeTaC films occurs at 500°C,

showing the strong  $\alpha$ -Fe (110) peaks. Compared with FeTaN films, two distinct features in the diffraction peak



(a)  $\text{Fe}_{78.8}\text{Ta}_{8.5}\text{N}_{12.7}$  films.



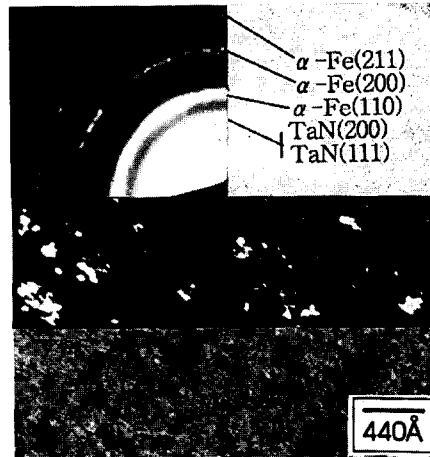
(b)  $\text{Fe}_{75.6}\text{Ta}_{8.1}\text{C}_{16.3}$  films.

Fig. 7. XRD diffraction patterns of FeTaN and FeTaC films annealed at various temperatures.

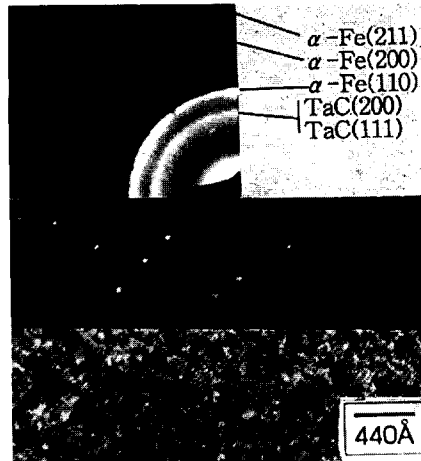
profiles can be recognized here. Firstly, broadening of  $\alpha$ -

Fe (110) peaks are relatively lower and peak profile is more symmetrical than in FeTaN films. These peak profiles suggest that the peak broadening mainly results from the particle size effect rather than the lattice expansion. Another feature is the strong hallow pattern which exists around  $30 \sim 43^\circ$  diffraction angles. The hallow pattern is considered to come from the presence of fine TaC particles. At  $700^\circ\text{C}$ , sharply defined  $\alpha$ -Fe,  $\text{TaC}_{0.47}$ ,  $\text{Fe}_3\text{C}$  peaks are observed. It is interesting to note that the TaC phases, which observed at  $500^\circ\text{C}$ , are transformed to  $\text{TaC}_{0.47}$  phases at this temperature. Detail mechanism for this transformation is not uncertain.

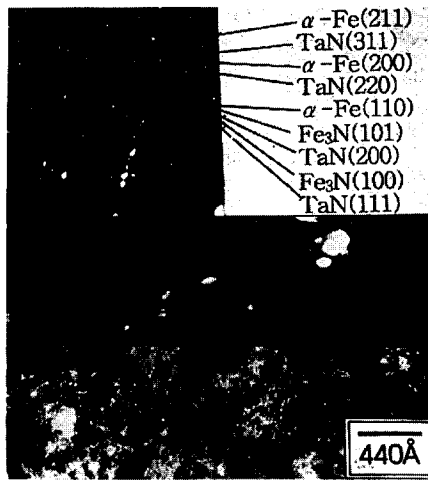
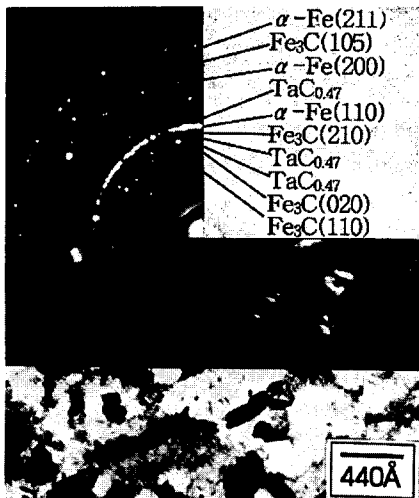
More detail information on the microstructure of



(a)  $\text{Fe}_{78.8}\text{Ta}_{8.5}\text{N}_{12.7}$  films, annealed at  $500^\circ\text{C}$ .



(b)  $\text{Fe}_{75.6}\text{Ta}_{8.1}\text{C}_{16.3}$  films, annealed at  $500^\circ\text{C}$ .

(c)  $\text{Fe}_{78.8}\text{Ta}_{8.5}\text{N}_{12.7}$  films, annealed at  $700^\circ\text{C}$ .(d)  $\text{Fe}_{75.6}\text{Ta}_{8.1}\text{C}_{16.3}$  films, annealed at  $700^\circ\text{C}$ .Photo. 1. TEM images and electron diffraction patterns of FeTaN and FeTaC films annealed at  $500^\circ\text{C}$  and  $700^\circ\text{C}$ .

films can be obtained by TEM studies. As-deposited films show amorphous structures in both FeTaN and FeTaC films. Fig. 8. is the TEM micrographs with SAD patterns for the microstructures FeTaN and FeTaC films annealed at  $500^\circ\text{C}$  and  $700^\circ\text{C}$ . At  $500^\circ\text{C}$ , both films show very fine  $\alpha$ -Fe grains with sizes of  $60\sim 70\text{\AA}$ , which are in agreement with XRD results. The distinguishable features of SAD patterns between FeTaC and FeTaN films annealed at  $500^\circ\text{C}$  are that TaC diffraction shows well defined ring pattern for FeTaC films, while TaN diffraction shows

broadened ring pattern in FeTaN films. These results suggest that some coarsening of TaC particles already occurs at this temperature in FeTaC films. Coarsening of the TaC particle will reduce the efficiency in impeding the grain growth of  $\alpha$ -Fe. The efficiency in impeding grain growth of TaN and TaC particles can be recognized in the films annealed at  $700^\circ\text{C}$ . The grain sizes of FeTaC films appear to be substantially larger than those of FeTaN films. It is noted that fine grains lead to good soft magnetic properties with low  $H_c$  and high  $m'$  values, the observed higher thermal stability of FeTaN films can be explained by higher efficiency of TaN particles in suppressing grain growth.

#### IV. CONCLUSIONS

The magnetic properties and microstructures of FeTa-N,C films were investigated, and the results can be summarized as follows.

- 1) The magnetic properties of FeTaN films with  $H_c : 0.25$  Oe,  $4\pi M_s : 14.5$  kG, and  $\mu' : 4000$  (5MHz) and FeTaC films with  $H_c : 0.25$  Oe,  $4\pi M_s : 14.5$  kG, and  $\mu' : 2700$  (5MHz) can be obtained.
- 2) The process range showing the good magnetic properties is larger in FeTaC films than in FeTaN films.
- 3) In both FeTaN and FeTaC films, the films show the best soft magnetic properties at showing the minimum grain sizes.
- 4) TaN particles in FeTaN films show higher efficiency in retarding the  $\alpha$ -Fe grain growth during heat treatments than TaC particles in FeTaC films, resulting in the higher thermal stability of FeTaN films.

#### REFERENCE

- [1] Y. Takeshima, N. Ishiwata, T. Korenari and H. Urai, J. Appl. Phys., 73(10), 6576 (1993).
- [2] N. Ishiwata, C. Wakabayashi and H. Urai, J. Appl. Phys. 69(8), 5616 (1991).
- [3] N. Hasegawa, M. Saito, A. Kosima, A. Makino, Y. Misaki and T. Watanabe, J. Magn. Soc. Jpn., 14, 319 (1990)
- [4] N. Hasegawa and M. Saito, J. Magn. Soc. Jpn., 14(2), 313 (1990).
- [5] M. Komuro, Y. Kozono, M. Hanazono and Y. Sugita, J. Magn. Soc. Jpn., 4(3), 547 (1990).
- [6] E. A. Brandes, "Smithells Metals Reference Book", Six Edition, P11-248.